Fine-grained Indoor Localization:

Visible Light Communication

M. Vieira, M. A. Vieira, P. Louro, A. Fantoni
ADETC/ISEL/IPL,
R. Conselheiro Emídio Navarro, 1959-007
Lisboa, Portugal
CTS-UNINOVA
Quinta da Torre, Monte da Caparica, 2829-516,
Caparica, Portugal

e-mail: mv@isel.ipl.pt, mv@isel.pt, plouro@deetc.isel.pt,
afantoni@deetc.isel.ipl.pt

P. Vieira
ADETC/ISEL/IPL,
R. Conselheiro Emídio Navarro, 1959-007
Lisboa, Portugal
Instituto das Telecomunicações
Instituto Superior Técnico, 1049-001,
Lisboa, Portugal
e-mail: pvieira@isel.pt

Abstract—**An indoor positioning system where trichromatic white Light Emitting Diodes (LEDs) are used both for illumination proposes and as transmitters and an optical processor, based on a-SiC:H technology, as mobile receiver is presented. On-Off Keying (OOK) modulation scheme is used, and it provides a good trade-off between system performance and implementation complexity. The relationship between the transmitted data and the received digital output levels is decoded. LED bulbs work as transmitters, sending information together with different identifiers, IDs, related to their physical locations. A triangular topology for the unit cell is analysed, and a 2D localization design, demonstrated by a prototype implementation, is presented. Fine-grained indoor localization is tested. The received signal is used in coded multiplexing techniques for supporting communications and navigation concomitantly on the same channel. The location and motion information is found by mapping the position and estimating the location areas**.

Keywords- a-SiC: H technology; optical sensor; transmitter; receiver; demultiplexer; WDM; indoor positioning.

I. INTRODUCTION

Research on indoor localization and navigation has long been a popular topic. Localization is one of the essential modules of many mobile wireless applications. Although Global Positioning System (GPS) works extremely well for an open-air localization, it does not perform effectively in indoor environments, due to the inability of GPS signals to penetrate through in-building materials. Therefore, precise indoor localization is still a critical missing component and has been gaining growing interest from a wide range of applications, e.g., location detection of assets in a warehouse, patient tracking inside the hospital, and emergency personnel positioning in a disaster area. Although many methods are available, such as WiFi-based [1], [2] and visual indoor topological localization [3], [4], they require dense coverage of WiFi access points or expensive sensors like high-performance cameras to guarantee the localization accuracy.

In the sequence, we propose to use modulated visible light (carried out by white low cost Red, Green, and Blue, RGB, LEDs) to provide globally consistent signal-patterns to perform indoor localization.

We present a 2D localization design, demonstrated by a prototype implementation. The main issue is to divide the space into spatial beams originating from the different light sources, and identify each beam with a unique time sequence of light signals. The receiver, equipped with a light sensor, determines its spatial beam by detecting the light signals, followed by optimization schemes to refine its location within the beam. Fine-grained indoor localization can enable a multitude of applications. In supermarkets and shopping malls, exact location of products can greatly improve the customer's shopping experience and enable customer analytics [5], [6].

Visible Light Communication (VLC) is a data transmission technology [7], [8], [9], and [10], based on the use of visible light. Due to the combination of illumination and communication, a lot of research has been performed for VLC applications [11], [12], and [13]. With this technology, it is possible to achieve simultaneous illumination and data transfer by means of LEDs. This functionality has given rise to VLC, where LED luminaires are used for high-speed data transfer [14], [15]. Moreover, both interior lighting of a room and data transfer will be achieved without the need of an additional communication system. Aside from integrability with the illumination system, VLC has many advantages compared with other radio based technologies: radio frequency (RF) interference free, RF interference immune, safe for human health, and more secure [16]. Luminaires equipped with multi colored LEDs can provide further possibilities for signal modulation and detection in VLC systems [17].

The use of Red-Green-Blue (RGB) LEDs is a promising solution to high-speed VLC systems as they offer the possibility of the Wavelength Division Multiplexing (WDM), which can greatly increase the transmission data rate. In the recent past, we have developed a WDM device

that enhances the transmission capacity of optical communications in the visible range. The device was based on tandem a-SiC:H/a-Si:H pin/pin light controlled filter with two optical gates that select the different channel wavelengths. When different visible signals are encoded in the same optical transmission path [18], [19] the device multiplexes the different optical channels, and performs different filtering processes: amplification, switching, and wavelength conversion. Finally, it decodes the encoded signals recovering the transmitted information.

This paper provides detailed characteristics of various components in a VLC system such as transmitter and receiver, multiplexing techniques, system design and visible light sensing and applications, such as indoor localization and motion recognition. A 2D localization design, demonstrated by a prototype implementation will be analyzed. Fine-grained indoor localization is tested. The proposed system, composed data transmission and indoor positioning, involves wireless communication, smart sensor and optical sources network, which constitutes a transdisciplinary approach framed in cyber-physical systems.

This paper is organized as follows. In Section I, an introduction is presented. In Section II, the system configuration and its characterization is explained. In Section III, indoor positioning is analyzed while, in Section IV, some navigation system examples are shown. Finally, Section V summarizes the conclusions.

II. SYSTEM CONFIGURATION AND CARACTERIZATION

A. Transmitter

The positioning system's topology is a self-positioning system in which the measuring unit is mobile. This unit receives the signals of several transmitters in known locations, and has the capability to compute their location based on the measured signals. LED bulbs work as transmitters, sending information together with different IDs related to their physical locations. Each LED lamp transmits data during the time slot it occupies, i.e., the individual LED lamp transmits its own data depending on the area it locates. An optical receiver inside the mobile terminal extracts the location information to perform positioning and, concomitantly, the transmitted data from each transmitter.

The beam area of light radiation of an LED, in the array, has the form of a circle. The estimate distance from the ceiling is used to generate a circle around each transmitter (see Figure 1) on which the device must be located in order to receive the transmitted information (generated location and coded data). To receive the information from several transmitters, the device must be positioned where the circles from each transmitter overlap, producing at the receiver a MUX signal that, after demultiplexing, acts twofold as a positioning system and also a data transmitter. The receiver detects one or more signals from light beams of different LEDs. If the signal it receives is only from one LED, the coordinates of the LED are assigned the device's reference point. If the device receives multiple signals, i.e., if it is in the overlapping region of two or more LEDs, it finds the centroid of the received coordinates and stores it as the

reference point. Thus, the overlap region is used as an advantage to increase the accuracy in position estimation because more overlapping region means more reference points.

The proposed system considers a set of LED bulbs on the ceiling and a mobile terminal. The ceiling plan for the LED array layout of a unit cell is shown in Figure 1a (LED array = RGBV color spots). A triangular topology was considered for the unit cell (Figure 1a). The proposed arrangement employs four modulated LEDs (RGBV), three of them (RGB-LED) are located at the vertices of an equilateral triangle and a fourth one (V) is located at its centroid. The geometric scenario used for calculation uses a calibration grid (triangular), smaller, to improve its practicality. Here, a beam radius of 2 cm was assumed for each LED. The chips of the white LEDs can be switched *on* and *off* individually in a desired bit sequence and are 3 cm away from the receiver. For each RGB-LED, only one chip (R, G, B) is modulated in order to broadcast the specific information (payload data). The extra violet LED sends the network cell's. We name point 1 where all the four locations overlap. Points 2, 3 and 4 refer to the locations with three overlaps, points 5, 6 and 7 with two overlaps, and finally 8, 9 and 10 where no overlap occurs. The grid size was chosen in order to have the triangle inscribed inside the generated circle estimated around the violet transmitter.
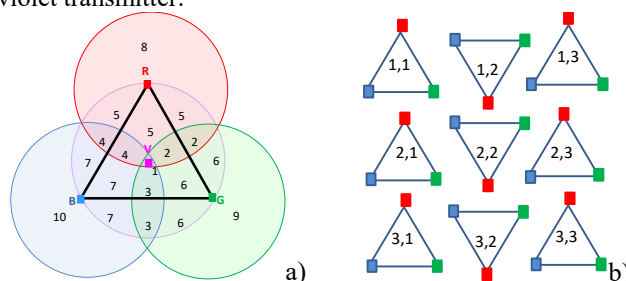

Figure 1. The next closest grid positions in lighting design. a) unit navigation cell. b) network cell's

The triangular topology allows the use of clusters cells and can be applied on large surfaces (Figure 1b). A large-dimension indoor environment, like a supermarket or a library can be considered by dividing the room into unit navigation cells with an appropriate side length. In Figure 1b, the unit cell was repeated in the horizontal and vertical directions in order to have a *mxn* matrix of unit cells that fill all the space and gives the geographical position assigned to each unit cell. The violet signal carries the ID of the unit cell. Cell's IDs are encoded as rows and columns [rrrr; cccc] using a binary representation for decimal number. For instance, number 11 is coded as "1011" ($2^3+0+2^1+2^0$). In case of the presented cell in Figure 1a being part of the cluster (Figure 1b) the ID from the cell located at row 1: column 1, will be [0001 0001], whereas in case of row 2 column 3, an ID_BIT [0010 0011] will be send by the violet LED. With perfect information, this method will give an exact, unique answer, i.e., the cell location in the cluster and for each unit navigation cell, the single region at the intersection of the circles.

As stated, the employment of trichromatic RGB LEDs as transmitters offers the possibility of WDM, which can greatly increase the transmission data rate.

Light produced by the LEDs is assumed to propagate as a Gaussian Beam. Under this assumption, in agreement with the LED's datasheet used for the laboratory experimental measurement, the electric field intensity propagates in free space in its unique fundamental mode [20]. Applying this model, we calculate the light intensity projected on the target screen based on the LED characteristics: wavelength, intensity and divergence angle (60º). In Figure 2, the simulation of the projected light intensities is shown for the unit triangular cell. The coordinates of the LEDs, in centimeters, were set as: V (0, 0), R (0, 2), B(-1.72, -1), G (1.72, -1).
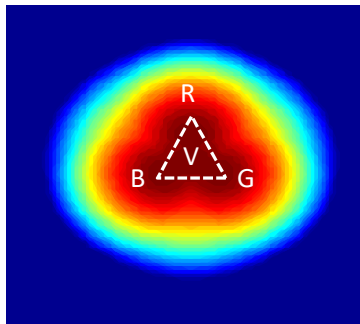

Figure 2.   Simulated light intensity in a triangular unit cell.

To transmit the data, an On-Off Keying (OOK) code was used. In Figure 3, an example of the digital signals (RGBV codeword) used to drive the LEDs is displayed. In this example, the ID_BIT [0101 0011] was sent by the violet LED and corresponds to the unit cell (5,3). The red, the green and the blue LED send the payload data.
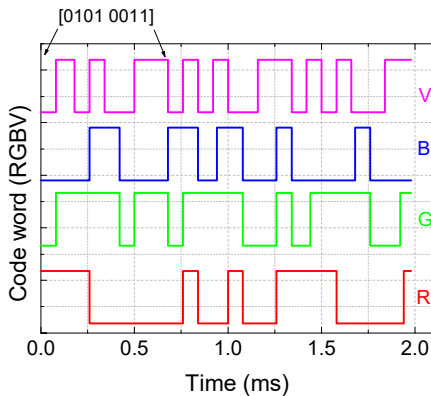

Figure 3.   Representation of the original encoded message [R G B V] ascribed to the cell (5,3).

B.   Receiver

The optoelectronic sensor is a 1x1 cm double pin heterostructure produced by PECVD (Plasma Enhanced Chemical Vapor Deposition) sandwiched between two transparent conductive contacts (TCO). The device configuration is shown in Figure 4. In the heterostructure, p-i'(a-SiC:H)-n/p-i(a-Si:H)-n [17], the intrinsic layer of the front p-i-n photodiode is built of a-SiC:H while the back intrinsic layer is based on a-Si:H. As a result, both front and back diodes act as optical filters confining, respectively, the optical carriers resultant from the blue and red wavelength photons apart, while the optical carriers generated by the green wavelength photons are absorbed across both.

The device operates within the visible range using for data transmission modulated low power light supplied by a violet (V), and three trichromatic LEDs. The RGB-LED are used together for illumination proposes and individually, one only chip, to transmit the channel location and data information. So, a polychromatic mixture of red, green, blue and violet; $\lambda_{R,G,B,V;}$ pulsed communication channels (input channels, transmitted data) are combined together, each one with a specific bit sequence and absorbed accordingly to their wavelengths (see arrow magnitudes in Figure 4). The combined optical signal (multiplexed signal; received data) is analyzed by reading out the generated photocurrent under negative applied voltage (-8V), with and without 390 nm background lighting, applied either from front or back sides [18].
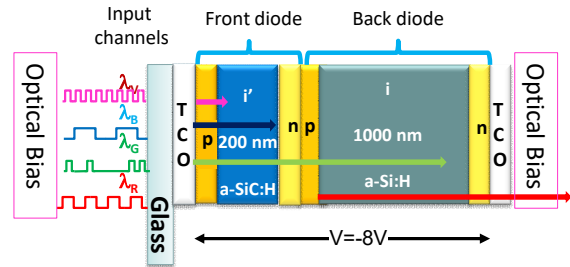

Figure 4.   Double pin configuration and device operation.

In Figure 5, the measured signal due to the overlap of the four independent input channels (MUX signal) is displayed without applied optical bias (dark) and under front and back irradiation. On the top the driving signal applied to each R, G, B and V LED is presented, the bit sequence was chosen in order that when one channel is *on* the others are always *off*.
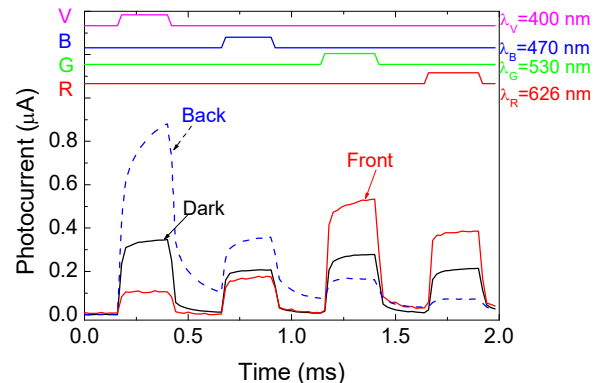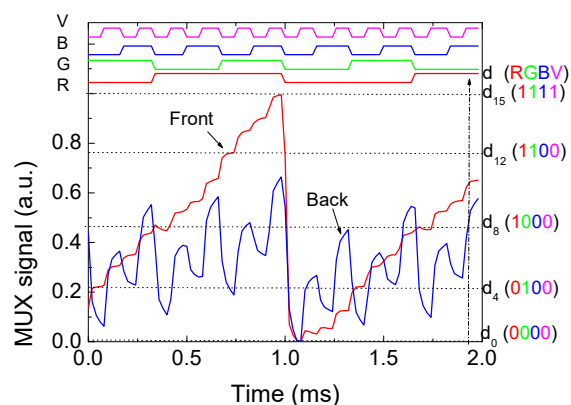

Figure 5.   Transient photocurrent without (Dark) and under front (Front) and back (Back) 390 nm irradiation.
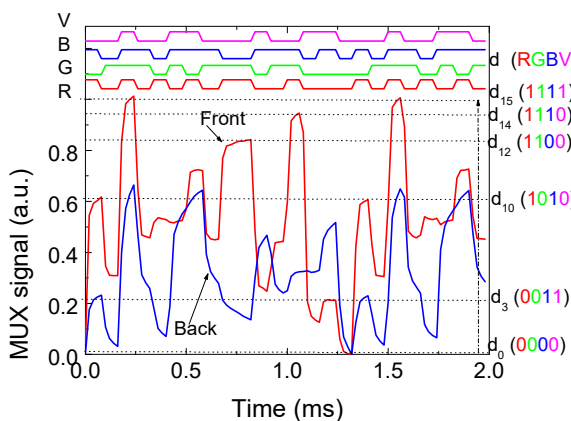
Data analysis shows that the photocurrent depends, under irradiation, on the irradiated side and on the incoming wavelength, the irradiation side acting as the optical selector for the input channels. Under front irradiation, the long wavelength channels are enhanced and the short wavelength channels quenched while the opposite occurs under back irradiation. Note that, under back lighting, as the wavelength increases the signal strongly decreases while the opposite occurs under front irradiation. This nonlinearity is the main idea for decoding the MUX signal at the receiver.

C. MUX/DEMUX device

For the unit cell, and with the receiver at position generation 1 (see Figure 1), the photocurrent generated by all the input channels was measured under front and back lighting.

Figure 6. MUX signal under front and back irradiation. On the top the transient optical signal from each RGBV are decoded.

The bit sequence of each channel was adjusted in order to have all the *on/off* possible states in an ordered sequence. The photocurrent was normalized to its maximum value. In Figure 6a this "standard" MUX signal is displayed, under front and back irradiation. In Figure 6b a random sequence is shown under the same conditions. In the top of the figures, the digital decoded information is shown.

The MUX signal under front irradiation is quite different from the one under back lighting. Results from the "standard" sequence (Figure 6a) show that for each possible 2^4 *on/off* states, it corresponds a well-defined level. Under front irradiation, sixteen separate levels are detected (d_0-d_{15}) and correspond to all possible combinations of the *on/off* states, concerning the input channels. Under back irradiation, the MUX signal trend is very close to the one of the violet input channel and allows the readout of the cell´s ID-BIT. In Figure 6b, some *on/off* states are missing, but, as expected, the behavior is the same: front irradiation enhances the red/green channels while under back irradiation the violet channel is readout.The functional principle to decode the transmitted information is based on the adjustable penetration depths of the photons into the front and back diodes (see Figure 4), which is linked to their absorption coefficient in the intrinsic front and back collection areas. Front irradiation is strongly absorbed at the beginning of the front diode and, due to the self-bias effect, increases the electric field at the back diode, where the red incoming photons are absorbed, resulting in an increased collection. Under back irradiation, the electric field decreases, mainly at the i-n back interface, quenching the red signals and enhancing the blue /violet ones (see Figure 5).

The algorithms to decode the coded information are relatively straight-forward since the background acts as selector that chooses one of the 2^n sublevels, being *n* the number of transmitted channels, and associates to each level an unique *n*-bit binary code [21]. The combination of the four channels under irradiation, denotes the presence of all the possible sixteen (2^4) *on/off* states, clearly observed in Figure 6a. Here, each level is ordered by the correspondent gains in a 4 bit binary code [X_R, X_G, X_B, X_V], with X=1 if the channel is *on* and X=0 if it is *off*. In Figure 6, in the right side, it is presented the selection index for the 16-element look-up (d_0-d_{15}) table, each one in its 4-bit binary code (RGBV) [18]. Therefore, by assigning each output level to a *n* digit binary code weighted by the optical gain of each channel, the signal can be decoded. A maximum transmission rate capability of 30 kbps was achieved in a four channel transmission using this device. In the top of the figure, the digital decoded information is shown.

III. INDOOR POSITIONING

In Figure 7, the MUX signals with the receiver at the nearest positions 2 and 6, under front lighting, are presented. In Figure 7a, the "standard" bit sequence (Figure 6a) was analyzed, while in Figure 7b, the random one (Figure 6b) was imposed.

Along *n* channel WDM message transmission, 2^n *on/off* states are possible during an interval of time T (see Figures 6 and 7). The position of the device during the receiving process will be given by the highest detected level, i. e., the level where all the *n* received channels are simultaneously *on* [22]. So, the four (RGBV, Figure 6), the three (RGV, Figure 7) or two (GV, Figure 7) received messages will be given by the decoding of the *n* received channels while the device

position will be confirmed by looking at the highest level (dot-dash line).
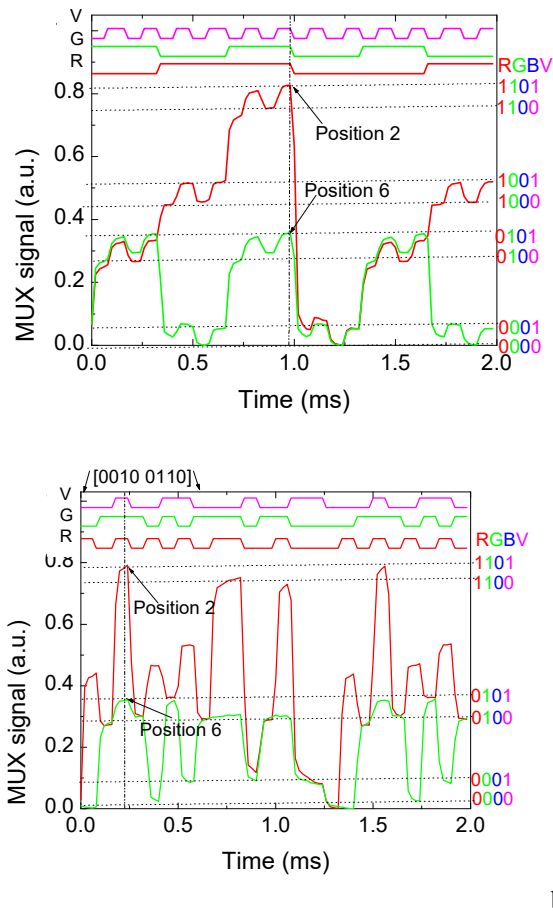

a)

b)

Figure 7.   MUX signals under 390 nm front and back irradiation. On the top the transmitted channels were decoded. a) Standard bit sequence. b) Random bit sequence.

The position ID for the analyzed examples will appear as [1111] (point generation 1, ([1111] in Figure 6) or [1101] (point generation 2, in Figure 7), and [0101], (point generation 6, in Figure 7). In Figure 7b, the eight first bits of the violet packet will give the 8-bit address of the unit cell, [0010 0110], that is located at line 2, column 6 from the network.

IV.   NAVIGATION DATA BITS

A challenge in LED-based navigation system is the way to improve the data transmission rate while maintaining the capability for accurate navigation. The input of the aided navigation system is the MUX signal, and the output is the system state estimated at each time step. For each transition between an initial location and a final one, two code words are generated, the initial (i) and the final (f). If the receiver stays under the same region, they should be the same, if it moves away they are different [23], [24].

The suitability of the navigation data bit transition was tested. The navigation solution is to move the sensor unit

along a known pattern path. One can performed signal acquisition on the different generated locations, for instance: beginning in point 5 and ending in point 3 (see Figure 1), in four consecutive instants (t_1, t_2, t_3 and t_4).

In a segment where the initial position of the receiver is point generation 5, then it moves to point 4, after that goes to point 7 and finally arrives to point 3, the acquired MUX signal at the instants t_1, t_2, t_3, and t_4 is displayed in Figure 8a. The decoded channels are depicted on top. On the right hand, the highest levels (horizontal dotted lines), in each time interval, and the correspondent code words are pointed out.
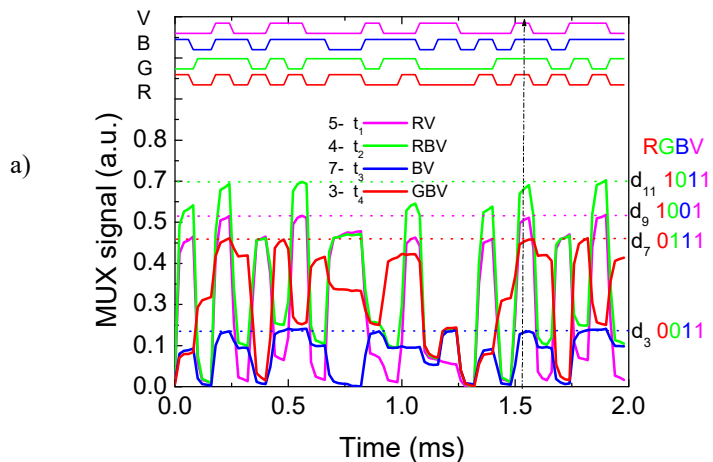

Figure 8.   Triangular topology. a) MUX/DEMUX signals under different generation regions (5, 4, 7, 3). b) Compass needle.

As the receiver moves between generated point regions, the received information changes. In turn, red, green or blue channels are added or removed, but the violet is always present giving the location of the cell inside the cluster. In the considered example, the 8-bit positioning ID decoded from the violet channel was [0010 0110], which corresponds to line 2, column 6 of the network. Hence, the retrieved information when the receiver was under point generation 4 (t_2) was: 8-bit positioning ID from the cell in the network [violet channel, 0010 0110], 4-bit positioning ID from the point generation cell: [RGBV, 1011], red channel payload packet: [1010 1010 1100 0100…]. When it moves to generation point 7 (t_3) the cell 4-bit positioning ID changes to [0011] the red information is lost and the blue payload data is maintained as: [1011 0111 0011 1010…]. Nevertheless, the 8-bit violet ID stays the same [0010 0110] since it corresponds to the same unit cell (line 2, column 6) in the network.

V.   CONCLUSION

This paper presents a coupled data transmission and indoor positioning by using transmitting trichromatic white LEDs and an a-SiC:H/a-Si:H pin/pin SiC optical MUX/DEMUX mobile receiver. For data transmission, an On-Off Keying code was used. A triangular topology was considered for the unit cell. The proposed arrangement employs four modulated LEDs. Three of them are located at

the vertices of an equilateral triangle to transmit the payload data and a fourth one is located at its centroid to send the positioning BIT ID from the unit cell in the network. Fine-grained indoor localization was tested. A 2D localization design, demonstrated by a prototype implementation was developed.

A detailed analysis of the component's characteristics within the VLC system, such as transmitter and receiver, multiplexing techniques, system design, visible light sensing, and indoor localization and navigation recognition were discussed. The results showed that, by using a pinpin double photodiode based on a a-SiC:H heterostucture as mobile receiver and RBG-LED as transmitters, it is possible not only to determine the position of a mobile target inside the unit cell but also in the network and concomitantly to infer the travel direction along the time. For future work, by using multiple emitters and receivers, the transmission data rate through parallelized spatial multiplexing can be improved.

REFERENCES

[1] Y. X. Sun, M. Liu, and Q. H. Meng, "Wifi signal strength-based robot indoor localization," in IEEE International Conference on Information and Automation, 2014.

[2] P. Bahl, and V. N. Padmanabhan, "Radar: an in-building rf-based user location and tracking system," in Proc. of IEEE INFOCOM, 2000.

[3] M. Liu, and R. Siegwart, "Dp-fact: Towards topological mapping and scene recognition with color for omnidirectional camera," in Robotics and Automation (ICRA), 2012 IEEE International Conference, may, pp. 3503 –3508, 2012.

[4] M. Liu, K. Qiu, S. Li, F. Che, L. Wu, and C. P. Yue "Towards indoor localization using visible light communication for consumer electronic devices," in Proceedings of the IEEE/RSJ International Conference on Intelligent Robots and Systems (IROS), Chicago, the USA, 2014.

[5] A. Jovicic, J. Li, and T. Richardson, "Visible light communication: opportunities, challenges and the path to market," Communications Magazine, IEEE, vol. 51, no. 12, pp. 26–32, 2013.

[6] S T. Komine and M. Nakagawa, "Fundamental analysis for visible-light communication system using led lights," Consumer Electronics, IEEE Transactions on, vol. 50, no. 1, pp. 100–107, 2004.

[7] E. Ozgur E. Dinc, and O. B. Akan, "Communicate to illuminate: State-of-the-art and research challenges for visible light communications," Physical Communication, no.17, pp. 72–85, 2015.

[8] J. Armstrong, Y. Sekercioglu, A. Neild, "Visible light positioning: a roadmap for international standardization," Communications IEEE, vol. 51, no. 12, pp. 68-73, 2013.

[9] K. Panta, and J. Armstrong, "Indoor localisation using white LEDs " Electron. Lett., vol. 48, no. 4, pp. 228–230, 2012.

[10] T. Komiyama, K. Kobayashi, K. Watanabe, T. Ohkubo, and Y. Kurihara, "Study of visible light communication system using RGB LED lights," in Proceedings of SICE Annual Conference, IEEE, pp. 1926–1928, 2011.

[11] Y. Wang, Y. Wang, N. Chi, J. Yu, and H. Shang. "Demonstration of 575-Mb/s downlink and 225-Mb/s uplink bi-directional SCM-WDM visible light communication using RGB LED and phosphor-based LED," Opt. Express vol. 21, no. 1, pp. 1203–1208, 2013.

[12] D. Tsonev, H. Chun, S. Rajbhandari, J. McKendry, S. Videv, E. Gu, M. Haji, S. Watson, A. Kelly, G. Faulkner, M. Dawson, H. Haas, and D. O'Brien, "A 3-Gb/s single-LED OFDM-based wireless VLC link using a Gallium Nitride µLED," IEEE Photon. Technol. Lett., vol.26 no.7, pp. 637–640, 2014.

[13] D. O'Brien, h. L. Minh, L. Zeng, G. Faulkner, K. Lee, D. Jung, Y. Oh, and E. T. Won, "Indoor visible light communications: challenges and prospects," Proc. SPIE 7091, 709106, 2008.

[14] S. Schmid, G. Corbellini, S. Mangold, and T. R. Gross, "An LED-to-LED Visible Light Communication system with software-based synchronization," in 2012 IEEE Globecom Workshops, pp. 1264–1268, 2012.

[15] Z. Zhou, M. Kavehrad, P. Deng, "Indoor positioning algorithm using light-emitting diode visible light communications " Opt. Eng. Vol.51, no. 8, 085009, 2012.

[16] S T. Komine and M. Nakagawa, "Fundamental analysis for visible-light communication system using led lights," Consumer Electronics, IEEE Transactions on, vol. 50, no. 1, 100–107, 2004.

[17] E. Monteiro, and S. Hranilovic, "Constellation design for color-shift keying using interior point methods," in Proc. IEEE Globecom Workshops, Dec., pp. 1224–1228, 2012.

[18] M. Vieira, P. Louro, M. Fernandes, M.A. Vieira, A. Fantoni and J. Costa, "Three Transducers Embedded into One Single SiC Photodetector: LSP Direct Image Sensor, Optical Amplifier and Demux Device," Advances in Photodiodes", InTech, Chap.19, pp. 403-425, 2011.

[19] M. A. Vieira, P. Louro, M. Vieira, A. Fantoni, and A. Steiger -Garção, "Light-activated amplification in Si-C tandem devices: A capacitive active filter model," IEEE sensor jornal, 12, no. 6, pp.1755-1762, 2012.

[20] E. A Saleh Bahaa and M. C. Teich, "Fundamentals of Photonics", John Wiley & Sons. Chapter 3, "Beam Optics," pp. 80–107, 1991.

[21] M. A. Vieira, M. Vieira, V. Silva, P. Louro, and M. Barata, "Optoelectronic logic functions using optical bias controlled SiC multilayer devices,". MRS Proceedings, vol. 1536, pp. 91-96, 2013.

[22] M. A. Vieira, M. Vieira, P. Louro, V. Silva, P. Vieira, "Optical signal processing for indoor positioning using a-SiCH technology," Opt. Eng. Vol. 55, no. 10, 107105, doi: 10.1117/1.OE.55.10, 2016.

[23] M. A. Vieira, M. Vieira, P. Louro, L. Mateus, and P. Vieira, "Indoor positioning system using a WDM device based on a-SiC:H technology," Journal of Luminescence, doi.:10.1016/j.jlumin.2016.10.005, 2016.

[24] P. Louro, J. Costa, M. A. Vieira, M. Vieira, "Optical Communication Applications based on white LEDs," J. Luminescence. doi.:10.1016/j.jlumin.2016.11.036, 2016.